DIFFERENTIAL SHRINKAGE IN NORMAL AND HIGH STRENGTH CONCRETE OVERLAYS

Johan Silfwerbrand, Assoc. Professor
Royal Institute of Technology
Dept. of Structural Engineering
S-100 44 Stockholm, Sweden

ABSTRACT

A simple method for calculation of shrinkage stresses in normal and high strength concrete overlays is proposed. Free shrinkage, creep, and degree of restraint are indata. Shrinkage can be measured easily by conventional test methods. A simple method for estimation of the creep coefficient is proposed. Equations for estimation of degree of restraint are derived. The method is used to estimate shrinkage stresses in normal strength concrete composite slabs and in concrete roads repaired with a high strength concrete overlay. The calculations show that the observed absence of cracking can be explained.

Key words: differential shrinkage, shrinkage stress estimations, shrinkage tests, creep tests, normal strength concrete, high strength concrete.

1. INTRODUCTION

Heavy traffic loads, de-icing salts, many freeze-thaw cycles, and in some countries an extensive use of studded tyres cause deterioration, wear, and rutting of concrete bridge decks and concrete pavements /1-3/. The unsound concrete has to be removed and replaced by new concrete. The repair results in a composite concrete structure. The new concrete overlay will shrink considerably, while the shrinkage of the base layer is negligible. The resulting differential shrinkage creates a loading case that must be accounted for /4-5/. In a composite structure, differential shrinkage leads to shrinkage stresses that are mainly compressive in the base layer and tensile in the overlay.

Calculation of shrinkage stresses is a very difficult task, because shrinkage, degree of restraint, modulus of elasticity, Poisson's ratio, creep, concrete age, and concrete quality all influence the stresses. Most of the factors are in turn dependent on concrete mix, temperature, humidity, and the dimensions of the structure. Creep and shrinkage prediction models are given in, e.g., ACI /6/, CEB /7/, and Bazant et al /8-14/. Due to the large number of influencing parameters, an accurate prediction of shrinkage stresses is almost impossible in an arbitrary case. The prediction is improved if creep and shrinkage estimations are based on tests on the actual concrete mix /14/. According to ACI /6/, the deviation between predicted and actual results decreases from ±30 % to ±15 %. Shrinkage and other material tests must be simple and the test results easy to use in the prediction model. In the following, an approximate and simple calculation method is derived and applied to two case studies.

2. ESTIMATION OF SHRINKAGE STRESSES

Consider a composite concrete beam composed of an old base and a new overlay (Fig. 1). The width of the beam is b, the total depth is b, and the depth of the overlay is αh. The modulus of elasticity of the overlay and the base is E_1 and $E_2=mE_1$, respectively. The following simplifications are introduced:

1) Concretes in base and overlay are linear elastic materials.
2) Poisson's ratio ν is set to zero.
3) Plane sections remain plane after bending (Bernoulli's bypothesis).
4) The shrinkage of the overlay is ε_{sh} throughout.
5) The shrinkage of the base is neglected.
6) A good bond between overlay and base provides complete interaction.
7) The beam edges are free to move (simply supported or free).

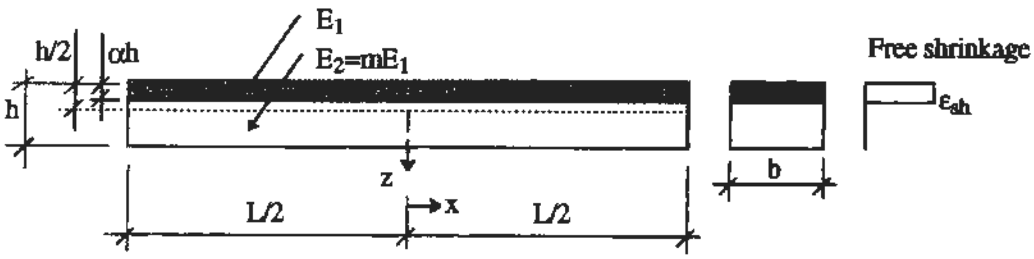

Fig. 1 *Composite concrete beam or slab.*

Shrinkage is usually higher at the top surface. The base might shrink slightly. The constant shrinkage distribution and the neglected base layer shrinkage lead, however, to a conservative prediction of shrinkage stresses. By using the engineer's $\nu=0$, shrinkage stresses in beams and slabs may be calculated with same formulae. For slabs on grade, friction between slab and subgrade is assumed to be low letting the slab to move horizontally without resistance. Friction is low for sustained loads and shrinkage stresses develop very slowly.

According to Bernoulli's hypothesis, the resulting strain $\varepsilon(z)$ in the beam can be given by the following expression:

$$\varepsilon(z) = \varepsilon_0 + \kappa \cdot z \quad (1)$$

where, z is a vertical coordinate with zero at mid depth of the beam, ε_0 is the strain at z=0, and κ is the curvature of the beam. The normal stress $\sigma(z)$ is given by the following expressions:

$$\sigma(z) = E_1(\varepsilon(z) + \varepsilon_{sh});\ -\tfrac{1}{2} \le z/h < \alpha-\tfrac{1}{2} \quad (2a)$$

$$\sigma(z) = mE_1\varepsilon(z);\ \alpha-\tfrac{1}{2} < z/h \le \tfrac{1}{2} \quad (2b)$$

Note that positive shrinkage is defined as a shortening, but positive strain is defined as an elongation. Positive stress is defined as a tensile stress.

The parameters ε_0 and κ can be determined by using the equations of equilibrium. Neglecting the dead load of the beam, both normal force N and bending moment M must vanish. By combining Eqs. (1) and (2), we obtain:

$$N = \int_{-h/2}^{-(\frac{1}{2}-\alpha)h} E_1(\varepsilon_0 + \kappa\cdot z + \varepsilon_{sh})b\cdot dz + \int_{-(\frac{1}{2}-\alpha)h}^{h/2} mE_1(\varepsilon_0 + \kappa\cdot z)b\cdot dz =$$

$$= E_1 b\cdot h\left([\alpha + m(1-\alpha)]\varepsilon_0 + (m-1)\alpha(1-\alpha)\frac{\kappa\cdot h}{2} + \alpha\cdot\varepsilon_{sh}\right) = 0 \qquad (3)$$

$$M = \int_{-h/2}^{-(\frac{1}{2}-\alpha)h} E_1(\varepsilon_0 + \kappa\cdot z + \varepsilon_{sh})b\cdot z\cdot dz + \int_{-(\frac{1}{2}-\alpha)h}^{h/2} mE_1(\varepsilon_0 + \kappa\cdot z)b\cdot z\cdot dz =$$

$$= \frac{E_1 b\cdot h^2}{2}\left((m-1)\alpha(1-\alpha)\varepsilon_0 + [m - (m-1)\alpha(3-6\alpha+4\alpha^2)]\frac{\kappa\cdot h}{6} - \alpha(1-\alpha)\cdot\varepsilon_{sh}\right) = 0 \qquad (4)$$

Solving Eqs. (3) and (4), we obtain the following values of ε_0 and κ:

$$\varepsilon_0 = \frac{-\alpha(m - (m-1)\alpha^3)}{m + (m-1)\{m(1-\alpha)^4 - \alpha^4\}}\cdot\varepsilon_{sh} \qquad (5)$$

$$\kappa = \frac{6\alpha(1-\alpha)m}{m + (m-1)\{m(1-\alpha)^4 - \alpha^4\}}\cdot\frac{\varepsilon_{sh}}{h} \qquad (6)$$

The maximum tensile stress σ_{max} in the overlay appears at the bottom of the overlay, i.e., at $z/h=\alpha-\frac{1}{2}$:

$$\sigma_{max} = \frac{m(1-\alpha)\{m(1-\alpha)^3 + \alpha^2(3+\alpha)\}}{m + (m-1)\{m(1-\alpha)^4 - \alpha^4\}}\cdot E_1\varepsilon_{sh} = \mu\cdot E_1\varepsilon_{sh} \qquad (7)$$

The coefficient μ expresses the degree of restraint and varies between 0 and 1 (Fig. 2). For the simple case m=1 and for $0.1<\alpha<0.9$, μ has a value close to 0.5. For thin and soft overlays (small α and large m values), μ approaches unity.

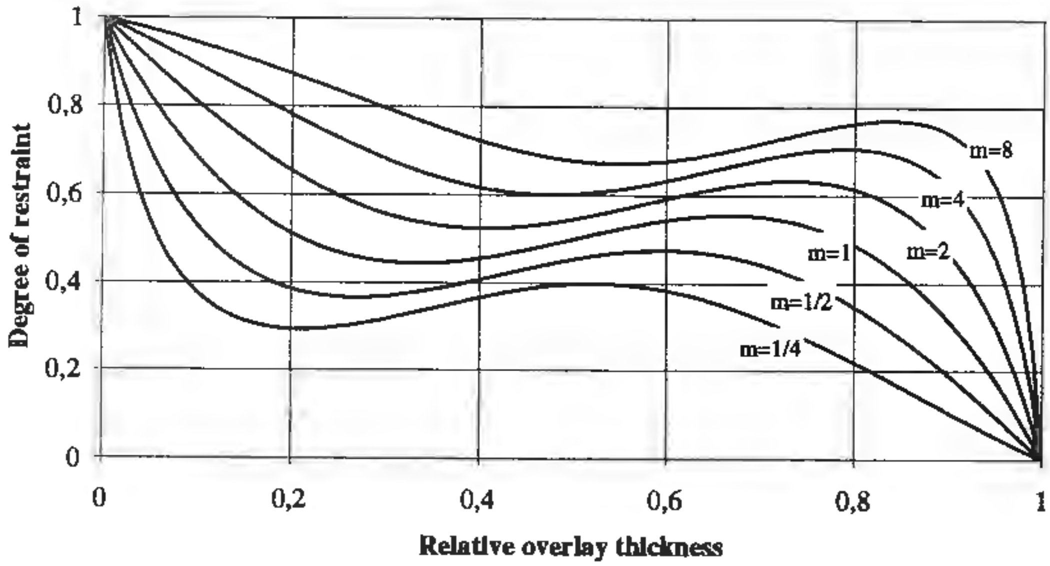

Fig. 2 *Degree of restraint* μ *as a function of relative overlay thickness* α *and stiffness ratios m between base and overlay.*

Concrete creep has a beneficial influence on the shrinkage stresses. Because shrinkage stresses develop during a rather long period, concrete creep will cause a considerable stress relief. (Compare with stress losses in prestressing steel due to stress relaxation). Concrete creep is higher at early ages and increases with increasing load duration and stress levels. Because each incremental shrinkage increase causes an incremental stress increase, accurate stress and strain analysis will be very complicated and time consuming for composite concrete structures subjected to differential shrinkage. If detailed knowledge of actual concrete properties and environmental effects is lacking, use of complicated models can hardly be motivated. Simple approximate methods taking both shrinkage and creep into account are desirable.

Concrete creep may be considered by introducing the creep coefficient ϕ. The relation between stress and strain can be given by the following expression:

$$\varepsilon = \frac{\sigma}{E} + \phi \cdot \frac{\sigma}{E} \qquad (8)$$

or

$$\sigma = \frac{E}{1+\phi} \cdot \varepsilon \qquad (9)$$

Hence, the modulus E of elasticity may be replaced by a fictitious modulus $E^*=E/(1+\phi)$.

We assume - conservatively - that the creep of the old base layer concrete is negligible. We denote the creep coefficient of the overlay concrete with ϕ. Assuming that the short time value of the modulus of elasticity is the same in base and overlay, we obtain $E_1^*=E/(1+\phi)$, $E_2^*=E_2=E$, and $m=E_2^*/E_1^*=1+\phi$. Finally, we obtain:

$$\sigma_{max} = \mu \cdot E_1{}^* \cdot \varepsilon_{sh} \quad (10)$$

Shrinkage stresses may now be estimated if shrinkage, creep coefficient, and modulus of elasticity are known. The best agreement between calculated and observed values are based on measurements on the actual concrete /14/. Measurements on creep and shrinkage are presented below.

3. TEST PROGRAMME

3.1 Test specimens and concrete

Tests were carried out on nine prisms. The prisms were 400×100×100 mm. Two types of concrete were tested: normal strength concrete and steel fibre reinforced high strength concrete. The first type was used for repairing concrete bridge decks. It was delivered in sacks as a pre-mixed dry mortar. Only water was added in the laboratory. The high strength concrete was mixed at the Swedish Cement and Concrete Institute copying a mix (also with steel fibres) that was used for repairing an old concrete pavement in southern Sweden. It may be stated here that moderate amount of steel fibres has only a little effect on shrinkage and creep /15/. Material data are given in Table 1.

Table 1 - Concrete data

	Normal strength concrete					High strength concrete			
Cement (kg/m^3)	420					430			
Aggregate 0-8 mm (kg/m^3)	-					800			
Aggregate 8-11 mm (kg/m^3)	-					950			
Aggregate 0-12 mm (kg/m^3)	Data lacking					-			
Water cement ratio	0.51					0.35 to 0.36			
Fibres (Dramix 30/0.5) (kg/m^3)	0					40			
Concrete age (days)	7	14	28	61	223	7	28	35	121
Compressive strength (MPa) on 150 mm cubes[1]	38	44	48	51	53	-	-	-	-
Compressive strength (MPa) on 150×300 mm cylinders[2]	-	-	-	-	-	62	78	74[5]	84
Splitting tensile strength (MPa) on 150 mm cubes[3]	3.2	2.8	3.2	3.1	3.0	-	-	-	-
Modulus of elasticity (GPa) on 150×300 cylinders[4]	-	-	-	-	-	-	-	42[5]	-

[1] Tested according to Swedish Standard SS 137210 (curing: 24 hours in air with RH=100 %, form removal, 4 days in water, remaining time in air with RH=37 %), [2] Tested according to SS 137230 (curing: 24 hours in air with RH=100 %, form removal, remaining time in water), [3] Tested according to SS 137213 (details on curing are missing), [4] Tested according to SS 137232 (curing: 24 hours in air with RH=100 %, form removal, remaining time in water), [5] Only one single specimen.

All prisms were stored in the Structural Engineering Laboratory at Royal Institute of Technology. In the beginning, they were moistened for seven days. During the remaining time, the prisms were exposed to the surrounding indoor climate described below.

The tests on normal strength concrete were carried out during the winter and spring of 1985-86. The temperature varied between +18 and +21°C. The relative humidity varied between 30 and 45 %. The average temperature and relative humidity were +20°C and 37 %, respectively.

The tests on high strength concrete were carried out during the spring of 1992. The temperature varied between +17 and +23°C. The relative humidity varied between 35 and 60 %. The average temperature and relative humidity were +19°C and 44 %, respectively.

3.2 Shrinkage tests

Concrete shrinkage was measured on four prisms made of normal strength concrete and on three prisms made of steel fibre reinforced high strength concrete. The prisms had the dimensions 400×100×100 mm. They were tested according to Swedish Standard SS 137215, where the shrinkage is defined as the ratio between the total shortening of the prism and the nominal prism length. The measurements started 7 days after casting, at the time of completed moistening. They were carried out during 6 months for the normal strength concrete and during 4 months for the high strength concrete. The final shrinkage was 0.6 and 0.45 mm/m, respectively (Figs. 3 and 4).

The measurement start at 7 days implies that the autogenous shrinkage during the first week could not be measured. This shrinkage is negligible for normal strength concrete. In high strength concrete, however, the autogenous shrinkage during the first week may be 0.05 to 0.10 mm/m (Persson /16/). The tested concrete had a water cement ratio of 0.35 (Table 1) limiting the probable autogenous shrinkage during the first week to 0.05 mm/m.

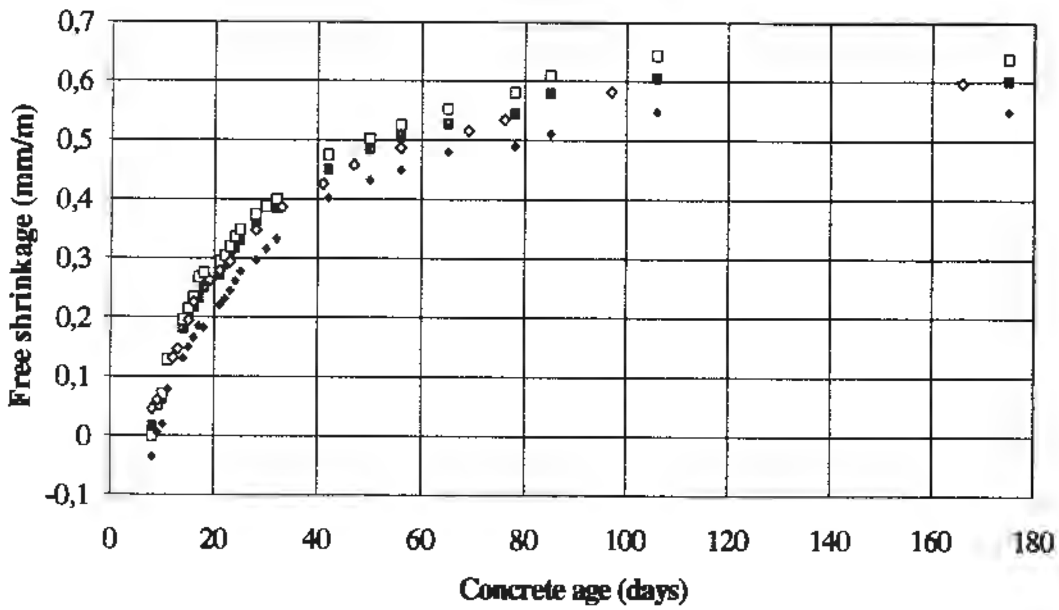

Fig. 3 *Measured free shrinkage on four test prisms of normal strength concrete. (White diamonds indicate the shrinkage of the prism used to evaluate creep tests. Black squares, white squares, and black diamonds indicate the shrinkage of prisms Nos. 1, 2, and 3, respectively).*

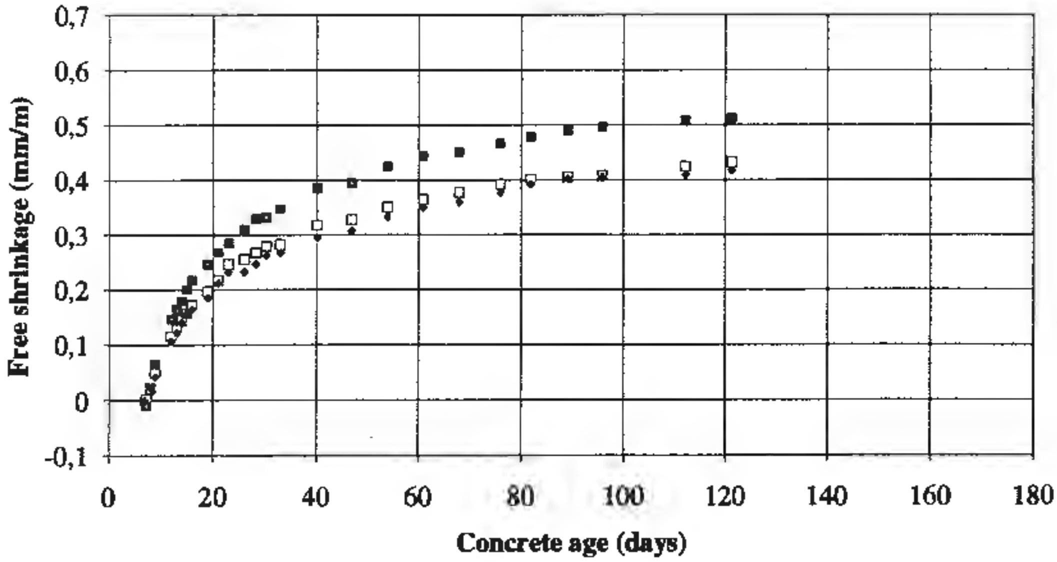

Fig. 4 *Measured free shrinkage on three test prisms of steel fibre reinforced high strength concrete. (Black squares, white squares, and black diamonds indicate the shrinkage of prisms Nos. 1, 2, and 3, respectively).*

3.3 Creep test method

Because concrete creep is dependent on both concrete age at loading t, load duration t'-t, and stress level σ/f (i.e., ratio between stress and strength), thorough creep tests are laborious, time consuming, and expensive. Creep data are here needed to calculate the effect of creep on shrinkage stresses. Because concrete shrinkage develops rapidly at early ages and slowly later (Figs. 3 and 4), shrinkage stresses are likely to follow the same pattern.

A creep test method has been developed in which the stress is increased in 5 MPa steps with short test periods in the beginning and long periods at the end (Fig. 5). Comparisons between shrinkage (Figs. 3 and 4) and loading history (Fig. 5) show an overall trend (both curves are continuously increasing, but with a decreasing rate). Consequently, evaluation of the creep observations should give a decent approximation of the creep influence on shrinkage stresses if we introduce two important assumptions: (i) the stress level and (ii) the stress sign (compression or tension) have negligible influence on creep.

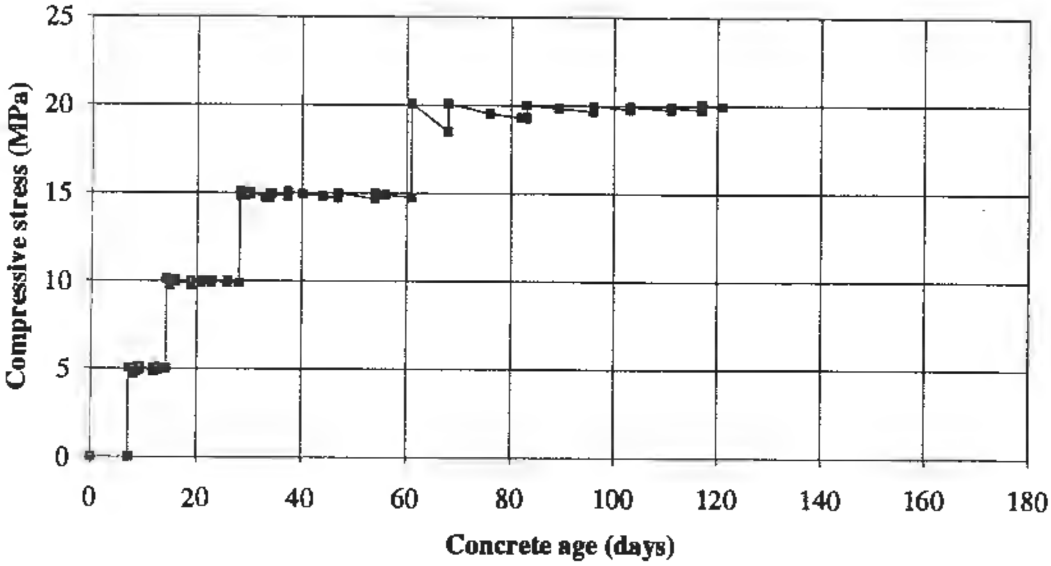

Fig. 5 *Loading history of creep test on steel fibre reinforced high strength concrete. (The different stresses correspond to approximately 6, 12, 19, and 25 %, respectively, of the compressive strength. A similar loading history - same stresses and loading days - was used for the test with the normal strength concrete).*

The creep data are found from tests on a concrete prism 400×100×100 mm that is loaded axially in compression. The load is produced by a heavy steel weight on a long lever arm (Fig. 6). The loading starts at t=7 days (time of completed moistening) and increases at 14, 28, and 61 days. The total shortening δ_{tot} is measured. The creep strain $\varepsilon_{cr}(t)$ can be computed by the following equation:

$$|\varepsilon_{cr}(t)| = \frac{\delta_{tot}(t)}{L} - |\varepsilon_{sh}(t)| - \frac{|\sigma(t)|}{E} \qquad (11)$$

where, $\varepsilon_{sh}(t)$ and $\sigma(t)$ is free shrinkage and compressive stress at time t, respectively, L is prism length (here; L=400 mm), and E is the modulus of elasticity (for simplicity, E is assumed to be independent of time). The stress is computed as the ratio between total load and cross sectional area (here; 100×100 = 10 000 mm^2). The modulus of elasticity can either be measured or estimated. The free shrinkage is measured on separate prisms made of the same concrete batch as the creep prism. Finally, the creep coefficient ϕ can be estimated as the ratio between creep strain ε_{cr} and elastic strain σ/E. We obtain:

$$\phi = \frac{\varepsilon_{cr}}{\sigma/E} \qquad (12)$$

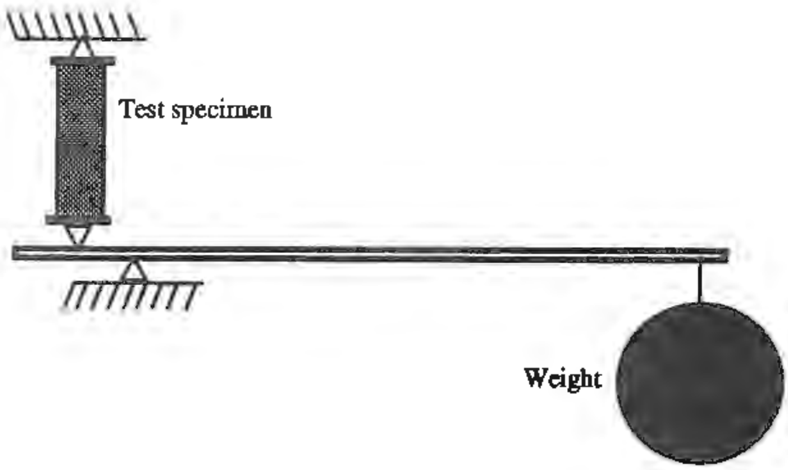

Fig. 6 *Creep test apparatus.*

3.4 Creep tests

One creep test was carried out on each type of concrete. For the test on normal strength concrete, free shrinkage was measured on a single prism cast from the same batch as the creep prism. The modulus of elasticity E was estimated to E=34 000 MPa through evaluation of the compressive tests on cubes. (The estimation was based on the relationship between modulus of elasticity and cylinder strength according to CEB-FIP MC 1990 /17/ and the relationship between cylinder and cube strength according to Swedish Standard SS 137207). For the tests on steel fibre reinforced high strength concrete, free shrinkage was measured on three prisms cast of the same batch as the creep prism. The average was used as free shrinkage. The modulus of elasticity was measured on a cylinder and estimated to E=42 000 MPa (Table 1).

The development of creep coefficient for normal and high strength concrete is shown in Figs. 7 and 8. After finished tests at four or five months, the creep coefficient was $\phi=3.7$ and $\phi=1.25$, respectively. The large difference in creep coefficient between normal and high strength concrete corresponds well to results from previous research /18-19/.

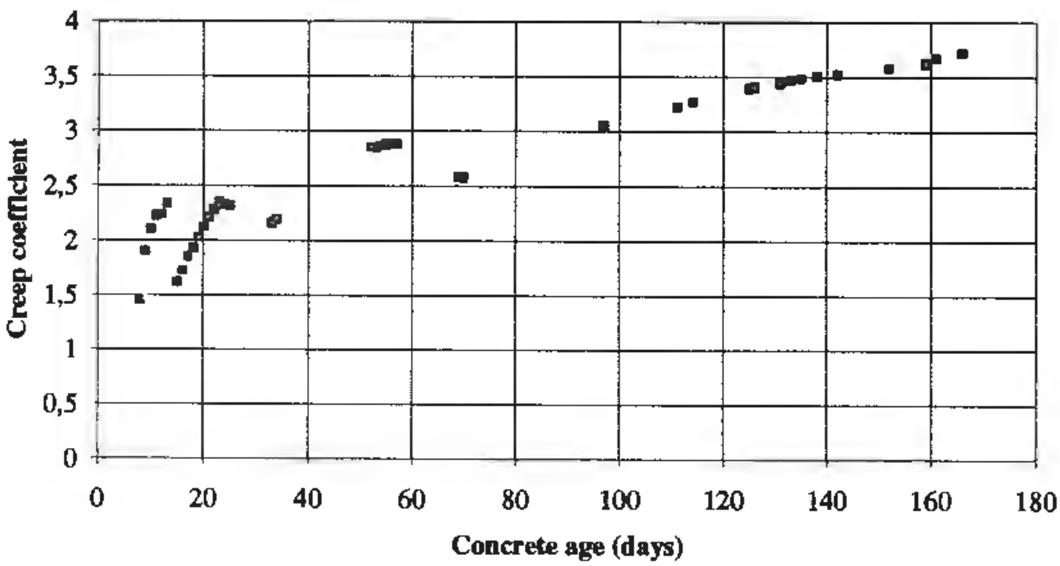

Fig. 7 *Creep coefficient defined as the ratio between creep strain and elastic strain obtained for normal strength concrete. (Loading history is shown in Fig. 5).*

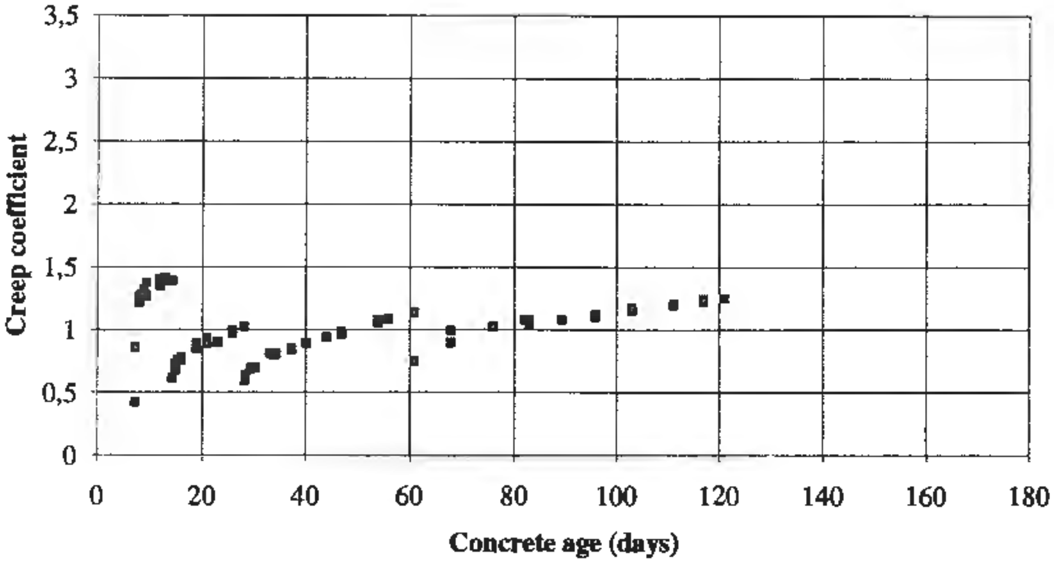

Fig. 8 *Creep coefficient defined as the ratio between creep strain and elastic strain obtained for steel fibre reinforced high strength concrete. (Loading history is shown in Fig. 5).*

4. CASE STUDIES

4.1 Laboratory tests on composite concrete slabs

Laboratory tests were carried out on five composite slabs /1/, /20/. The composite slab overlays were cast seven months after the concrete base layer. The overlay was cast with the normal strength concrete used for the shrinkage and creep tests reported above (Table 1). The concrete used for the base layer had a water cement ratio of 0.56, a cement content of 275 kg/m^3, and a maximum aggregate size of 32 mm. At time of finished test (after 450 days), the compressive cube strength was 52 MPa. The slabs were 2 m square (Fig. 9). The total thickness of the slabs was 150 mm. The ratio α between the overlay and the total thickness was 1/3.

Effects of differential shrinkage were studied during 6 months. No cracks were observed neither in the overlay nor in the interface between overlay and base.

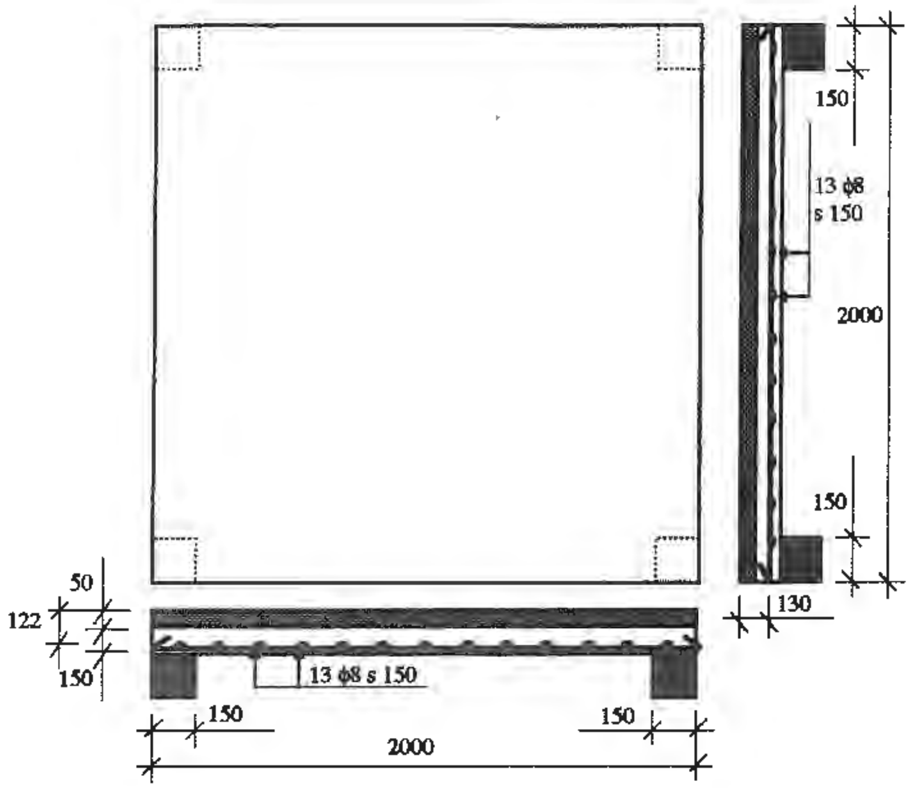

Fig. 9 *Tests on corner supported composite concrete slabs /20/. Measurements in mm.*

4.2 Field tests on overlaid concrete pavements

In 1978, a 7 km long concrete pavement was built in the south of Sweden. The road has two lanes in each direction. The plain jointed concrete pavement consists of a 200 mm thick concrete layer on top of a 150 mm thick cement bound roadbase. The distance between the transverse joints is 5 m. A longitudinal joint separates the high speed lane and the low speed lane. In 1991, the rutting depth was around 15 mm on the low speed lane. On a 475 m long test section, concrete was removed from the low speed lane and replaced by a 35 mm thick steel fibre reinforced high strength concrete overlay (Fig. 10) /2/. A similar concrete mix was later used in the shrinkage and creep tests discussed above (Table 1). Data of the old concrete is missing, but concrete pavements placed in the late 70s have usually a compressive strength of 40-50 MPa, and a modulus of elasticity about 30 000 MPa. After four years, no cracking has been observed by the local road administration /21/.

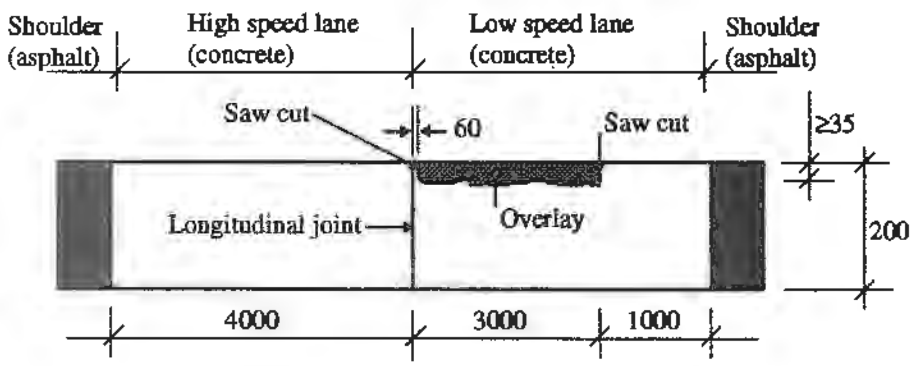

Fig. 10 *Field test on overlaid concrete pavement /2/. Measurements in mm. Note: the depth scale is exaggerated.*

4.3 Estimation of shrinkage stresses

Shrinkage stresses due to differential shrinkage have been estimated for both case studies. Conservatively, creep and shrinkage of the base layer have been neglected. By setting Poisson's ratio ν=0, the slabs may be treated as beams, and, thus, current equations derived for beams may be used. The calculations are summarised in Table 2. Values on free shrinkage and creep coefficients are taken from Figs. 3-4 and 7-8, respectively. Degree of restraint is given by Eq. (7) and maximum tensile stress in the overlay by Eq. (10).

Table 2 - Calculation of shrinkage stresses

Case study	Composite slabs				Overlaid pavement		
Overlay concrete	Normal strength				High strength		
Steel fibre content (kg/m^3)	0				40		
Ratio between overlay and overall thickness α	0.333				0.175		
E-modulus of overlay E_1 (GPa)	34				42		
E-modulus of base E_2 (GPa)	34				30		
Age of overlay t (days)	28	60	120	180	28	60	120
Free shrinkage ε_{sh} of overlay (mm/m)	0.35	0.50	0.60	0.60	0.28	0.38	0.45
Creep coefficient $\phi(t)$	2.3	2.9	3.3	3.7	1.03	1.13	1.25
Fictitious E-modulus of overlay $E_1^*=E_1/[1+\phi(t)]$ (GPa)	10.3	8.7	7.9	7.2	20.7	19.7	18.7
Fictitious E-modulus of base $E_2^*=E_2$ (GPa)	34	34	34	34	30	30	30
Stiffness ratio $m=E_2^*/E_1^*$	3.3	3.9	4.3	4.7	1.45	1.52	1.60
Degree of restraint μ	0.622	0.651	0.668	0.683	0.622	0.632	0.643
Maximum tensile stress in overlay σ_{max} (MPa)	2.24	2.83	3.17	2.95	3.61	4.73	5.41

Comparing tensile stresses (Table 2) with tensile strength (Table 1), we find that the stresses in the composite concrete test slabs are approximately the same as the available splitting tensile strength (about 3 MPa). The observed absence of cracking implies that the actual stresses have been lower than actual strength. Because the overlay tensile stress is not uniform, but decreases from the interface, it might be appropriate to use the flexural strength instead of the uniaxial tensile strength. The fact that the flexural strength usually is higher than the splitting tensile strength may be why cracks did not arise. It is interesting that the tensile stress decreases from a peak value at t=120 days. This calculation result agrees with the experience that shrinkage cracks are most likely to arise within a couple of months after concrete placement /22/.

For the steel fibre reinforced high strength concrete overlay, the computed stresses are higher (around 5 MPa) than the stresses in the normal strength concrete slabs. Tensile strength was not measured, but the measured compressive strengths indicate a flexural tensile strength of 6 MPa. The observed absence of cracking implies that such a strength has been sufficient. It may be added that non-measured autogenous shrinkage during the first 7 days of moistening (estimated to 0.05 mm/m, see subsection 3.2) may have introduced early stresses. Apparently, the sum of these stresses and the stresses due to drying shrinkage have been lower than available strength.

5. CONCLUDING REMARKS

Differential shrinkage causes stresses in repaired concrete structures. A simple calculation method for estimation of the risk of cracking is suggested. Shrinkage, creep, and degree of restraint are necessary indata. Shrinkage can be measured easily using conventional test methods. A simplified creep test method has been proposed. Equations for estimation of restraint are derived. The proposed method is used to estimate shrinkage stresses in composite laboratory test slabs and in an overlaid concrete road. Both normal and high strength concrete are considered. The calculations show that the shrinkage stresses in the overlay are somewhat lower than its flexural strength. Cracks have not been observed either. Furthermore, the calculations show that the risk of cracking increases during the first two months, but decreases subsequently.

6. ACKNOWLEDGEMENT

Financial support from the Swedish National Road Administration, the Development Fund of Swedish Construction Industry, and Cementa AB is gratefully acknowledged.

7. REFERENCES

/1/ Silfwerbrand, J., "Improving Concrete Bond in Repaired Bridge Decks," *Concrete International*, V. 12, No. 9, September 1990, pp. 61-66.

/2/ Silfwerbrand, J., and Petersson, Ö., "Thin Concrete Inlays on Old Concrete Roads," *Proceedings, 5th International Conference on Concrete Pavement Design & Rehabilitation*, Purdue University in West Lafayette, Indiana, USA, April 1993, V. 2, pp. 255-260.

/3/ Ingvarsson, H., and Westerberg, B., "Operation and Maintenance of Bridges and other Bearing Structures - State-of-the-Art Report and R&D Needs," *Bulletin* No. 42, Swedish Road and Traffic Research Institute, Linköping, 1986, 116 pp.

/4/ Birkeland, H.W., "Differential Shrinkage in Composite Beams," ACI JOURNAL, *Proceedings* V. 56, No. 11, May 1960, pp. 1123-1146.

/5/ Evans, R.H., and Chang, H.W., "Shrinkage and Deflection of Composite Prestressed Concrete Beams," *Concrete*, May 1967, pp. 157-166.

/6/ ACI Committee 209, "Prediction of Creep, Shrinkage, and Temperature Effects in Concrete Structures" (ACI 209R-92), American Concrete Institute, Detroit, 1992, 47 pp.

/7/ Comité Euro-International du Béton (CEB), "Structural Effects of Time-Dependent Behaviour of Concrete," Lausanne, 1984, 391 pp.

/8/ Bazant, Z.P., Kim, J.K., and Panula, L., "Improved Prediction Model for Time-Dependent Deformations of Concrete: Part 1 - Shrinkage," *Materials and Structures*, 1991, V. 24, pp. 327-345.

/9/ Bazant, Z.P., and Kim, J.K., "Improved Prediction Model for Time-Dependent Deformations of Concrete: Part 2 - Basic Creep," *Materials and Structures*, 1991, V. 24, pp. 409-421.

/10/ Bazant, Z.P., and Kim, J.K., "Improved Prediction Model for Time-Dependent Deformations of Concrete: Part 3 - Creep at Drying," *Materials and Structures*, 1992, V. 25, pp. 21-28.

/11/ Bazant, Z.P., and Kim, J.K., "Improved Prediction Model for Time-Dependent Deformations of Concrete: Part 4 - Temperature Effects," *Materials and Structures*, 1992, V. 25, pp. 84-94.

/12/ Bazant, Z.P., and Kim, J.K., "Improved Prediction Model for Time-Dependent Deformations of Concrete: Part 5 - Cyclic Load and Cyclic Humidity," *Materials and Structures*, 1992, V. 25, pp. 163-169.

/13/ Bazant, Z.P., Panula, L., Kim, J.K., and Xi, Y., "Improved Prediction Model for Time-Dependent Deformations of Concrete: Part 6 - Simplified Code-Type Formulation," *Materials and Structures*, 1992, V. 25, pp. 219-223.

/14/ Bazant, Z.P., Xi, Y., and Baweja, S., "Improved Prediction Model for Time-Dependent Deformations of Concrete: Part 7 - Short Form of BP-KX Model, Statistics, and Extrapolation of Short-Time Data," *Materials and Structures*, 1993, V. 26, pp. 567-574.

/15/ ACI Committee 544, "Design Considerations for Steel Fiber Reinforced Concrete," *ACI Structural Journal*, V. 85, No. 5, September 1988, pp. 563-580.

/16/ Persson, B., "Autogenous Shrinkage in High Performance Concrete," *Betong*, No. 2, May 1994, pp. 17-20. (In Swedish).

/17/ Comité Euro-International du Béton (CEB) and Fédération Internationale de la Précontrainte (FIP), "CEB-FIP Model Code 1990," 1990.

/18/ Nilson, A.H., "High Strength Concrete - An Overview of Cornell Research," *Proceedings, Symposium on Utilisation of High Strength Concrete*, Stavanger, Norway, June 15-17, 1987, pp.27-38.

/19/ Penttala, V., and Rautanen, T., "Microporosity, Creep, and Shrinkage of High-Strength Concretes," *Proceedings, Second International Symposium on High-Strength Concrete*, Berkeley, California, USA, May 1990, American Concrete Institute, SP-121, pp. 409-432.

/20/ Silfwerbrand, J., "Effects of Differential Shrinkage, Creep an Properties of the Contact Surface on the Strength of Composite Concrete Slabs of Old and New Concrete," *Bulletin* No. 147, Dept. of Structural Mechanics and Engineering, Royal Institute of Technology, Stockholm, Sweden, 1987, 131 pp. (In Swedish).

/21/ Fagergren, P., Unpublished correspondence between P. Fagergren at the Swedish National Road Administration in Malmö and the author, March 1996.

/22/ Concrete Society, "Non-Structural Cracks in Concrete," *Technical Report,* No. 2, 3rd Edition, The Concrete Society, Wexham, Slough, UK, 1992, 48 pp.